Computer simulations of dynamics of flux lines in type-II superconductors

Ryuzo Kato

Department of Applied Physics, Nagoya University, Nagoya 464-01, Japan

Yoshihisa Enomoto

Department of Physics, Nagoya University, Nagoya 464-01, Japan

Sadamichi Maekawa

Department of Applied Physics, Nagoya University, Nagoya 464-01, Japan

(Received 15 April 1991)

A method for studying the static and dynamical properties in the superconducting state is proposed, based on computer simulations of the solution of the time-dependent Ginzburg-Landau equation. We examine the dynamics of flux (vortex) lines in type-II superconducting films. It is shown that the nucleation of the superconducting state involves the formation of vortices and antivortices and their annihilation processes, even without an external magnetic field. We also show numerically how a flux line is trapped by a pinning potential.

I. INTRODUCTION

Since the discovery of high-T_c superconductors,[1] there has been a growing interest in the dynamics of flux (vortex) lines in type-II superconductors.[2] This is partly because the dynamics is pronounced in superconductors with a high transition temperature (T_c) and an experimental study of the dynamics is relatively easy. We also note that the dynamics of vortices is important for the technological applications of superconductors. Recently, various interesting properties of vortices have been experimentally studied in the high-T_c superconductors,[2] whereas theoretical study is still in the early stage.

It is known that the time-dependent Ginzberg-Landau (TDGL) equation is one of the most useful tools for studying the dynamics of superconductors. In this paper we propose a method of computer simulations for solving the TDGL equation in various physical situations. By introducing a gauge transformation of the vector and scalar potentials, the equation can be integrated numerically and the static and dynamical properties are simulated.

In Sec. II, we present a method for computer simulations for the solutions of the TDGL equation. In Sec. III, the method is applied to the nucleation problem of the superconducting states with and without an external magnetic field in a thin film, starting with the normal state, which is a nonequilibrium state below T_c. We examine the time development of the nucleation process, and observe that the process involves the formation of vortices and antivortices and their annihilation. The result shows that the phase fluctuation of the superconducting order parameter occurs more easily than that of the amplitude. In a magnetic field perpendicular to the film, a vortex lattice is stabilized. We extend our simulations to systems with a pinning center and study how a vortex is trapped by the center. In Sec. IV, we summarize our simulations and discuss a further extension of our method. Recently, several simulations of vortex states have been presented.[3-6] We present here simulations of the dynamics of the order parameter.

II. TIME-DEPENDENT GINZBURG-LANDAU EQUATION

The time-dependent Ginzburg-Landau equation provides a physical picture of the dynamics of superconductors in a magnetic field.[7] It is a partial differential equation for the space and time dependence of the complex order parameter Δ. The TDGL equation is conveniently written in the normalized form adapted by Hu and Thompson[8] as

$$D^{-1}\left[\frac{\partial}{\partial t}+i\frac{2e\psi}{\hbar}\right]\Delta+\xi^{-2}(|\Delta|^2-1)\Delta+\left[\frac{\nabla}{i}-\frac{2e}{\hbar c}\mathbf{A}\right]^2\Delta=0 ,$$

$$\mathbf{j}=\sigma\left[-\nabla\psi-\frac{1}{c}\frac{\partial\mathbf{A}}{\partial t}\right]+\mathrm{Re}\left[\Delta^*\left[\frac{\nabla}{i}-\frac{2e}{\hbar c}\mathbf{A}\right]\Delta\right]\frac{\hbar c^2}{8\pi e\lambda^2} ,$$

(1)

where $\mathbf{A}$ and ψ are the vector and scalar potentials in the normal state, respectively, and $\mathbf{j}$ is the current density. D and σ are the normal-state diffusion constant and conductivity, respectively, and have the relation,

$$\sigma = \frac{c^2\xi^2}{48\pi\lambda^2}\frac{1}{D} \ . \tag{2}$$

Here, ξ is the coherence length and λ is the magnetic penetration depth. The other notations are the conventional ones. In the above TDGL equation, the effects of the thermal fluctuation are neglected. The effect of temperature is introduced only through phenomenological parameters such as ξ, λ, and so on. The TDGL equation is solved together with the Maxwell equations

$$\mathbf{j} = \frac{c}{4\pi}\nabla\times(\nabla\times\mathbf{A}) \ ,$$

$$\mathbf{E} = -\frac{1}{c}\frac{\partial\mathbf{A}}{\partial t} - \nabla\psi \ , \tag{3}$$

$$\mathbf{B} = \nabla\times\mathbf{A} \ ,$$

with $\mathbf{E}$ and $\mathbf{B}$ being the electric field and the magnetic flux density, respectively.

Gor'kov and Eliashberg[9] derived the TDGL equation from the microscopic theory. They found that the equation is valid only for a gapless superconductor because of the singularity in the density of states at the gap edge. Moreover, the equation necessarily assumes that heating effects due to the dissipation of energy by the time-varying field and currents can be neglected. As Gor'kov and Eliashberg remarked, this restricts the applicability of the theory to very near T_c unless there is a very high density of paramagnetic impurities. However, for simplicity, throughout the present paper we regard the TDGL equations as the fundamental one to discuss the magnetic flux structures.

Let us introduce a gauge transformation of scalar and vector potentials

$$\mathbf{A}\rightarrow\mathbf{A}-\nabla\chi \ , \quad \psi\rightarrow\psi+\frac{1}{c}\frac{\partial\chi}{\partial t} \ , \tag{4}$$

accompanied by a phase redefinition of the order parameter

$$\Delta\rightarrow\Delta\exp\left[-i\frac{2e}{\hbar c}\chi\right] \ . \tag{5}$$

The gauge transformation leaves Eqs. (1) and (3) unchanged. It means that the physical results are independent of the choice of χ. Thus, in order to make the scalar potential zero, we set $\partial\chi/\partial t = -c\psi$. Then, the equations can be rescaled as follows:

$\mathbf{r}$ in units of $l\equiv\dfrac{\xi}{a}$,

t in units of $\dfrac{t_{GL}}{12}$,

$\mathbf{A}$ in units of $\sqrt{2}H_c\kappa l$,

ψ in units of $\dfrac{\hbar}{2et_{GL}}$, $\qquad(6)$

where H_c is the thermodynamic critical magnetic field. Here, a is a positive constant, which is afterward defined so as to make the numerical calculation efficient, t_{GL} and κ are, respectively, defined by

$$t_{GL} \equiv \frac{\pi\hbar}{8k_B(T_c-T)} \ ,$$

$$\kappa \equiv \frac{\lambda}{\xi} \ . \tag{7}$$

In the normalized units, the TDGL equation is rewritten as

$$\frac{\partial\Delta}{\partial t} = -\frac{1}{12}\left[\left[\frac{a}{i}\nabla - \frac{\mathbf{A}}{a}\right]^2\Delta + (|\Delta|^2-1)\Delta\right] \ ,$$

$$\frac{\partial\mathbf{A}}{\partial t} = \frac{a^2}{2i}(\Delta^*\nabla\Delta - \Delta\nabla\Delta^*) - |\Delta|^2\mathbf{A} - \kappa^2 a^2\nabla\times\nabla\times\mathbf{A} \ . \tag{8}$$

Note that Eq. (8) includes only two parameters κ and a since the variables $\mathbf{r}$, t, $\mathbf{A}$, and Δ are rescaled by the temperature-dependent quantities.

In the following, we consider a thin film of a type-II superconductor $(\kappa > 1/\sqrt{2})$ in the x-y plane with a magnetic field in the z direction. We are interested in the field configuration invariant along the z axis. Thus, the field depends only on the coordinates x and y, and the third component of the field is neglected. This situation may be physically realized if the thickness of the film, d, is much greater than the coherence length ξ and less than the penetration depth λ; that is, $d \lesssim \lambda$.

The outline of the procedure of the present simulation is as follows. First we discretize the TDGL equation and define it on a square lattice with N^2 lattice points. In our simulations, we use the simple Euler method with time step $\Delta t = 0.05$, the space step $\Delta x = \Delta y = 1$, and $a = 2$. The grid size is 60×60 $(N = 60)$, and so the space size is $30\xi\times 30\xi$ in physical units. We divide the complex oreder parameter Δ into real and imaginary parts. We also set $\kappa = 2$. In the normalized units the upper critical magnetic field is given by $H_{c2} = 1$ and the numerical value for the lower critical magnetic field H_{c1} is equal to 0.083 in our computer simulations, while this value may be compared with the expression $H_{c1} \approx \ln\kappa/2\kappa^2 = 0.087$ in the limit of large κ.

Periodic and free boundary conditions are introduced in the x and y directions, respectively. Therefore, at the film edge in the y direction, we have

$$\left[\frac{a}{i}\nabla - \frac{\mathbf{A}}{a}\right]\Delta\bigg|_n = 0 \tag{9}$$

for the order parameter where the suffix n denotes the normal direction at the boundary, and

$$\nabla\times\mathbf{A} = \mathbf{H}_e \ , \tag{10}$$

for the vector potential where $\mathbf{H}_e$ is the external magnetic field, which is applied along the z direction, $\hat{\mathbf{z}}$, is given by $\mathbf{H}_e = h_e(x,y)\hat{\mathbf{z}}$. These boundary conditions are concretely written as

$$\Delta(0,y) = \Delta(N,y) \ ,$$

$$A_x(0,y) = A_x(N,y) \ ,$$

$$A_y(0,y) = A_y(N,y) \ ,$$

$$\Delta(x,0) = \Delta(x,2) + i\frac{2}{a^2} A_y(x,1)\Delta(x,1) \ ,$$
(11)

$$A_x(x,0) = A_x(x,2) + 2h_e \ ,$$

$$A_y(x,0) = A_y(x,2) \ .$$

Initially, at each lattice site both real and imaginary parts of the order parameter are chosen to be different Gaussian random numbers with average 0 and variance 0.01, respectively, while we set $\mathbf{A} = (A_x, A_y) = (0,0)$.

Before studying the complicated situations, we first check the range of validity of our simulations using the analytic stationary solution of the TDGL equation.[7] We confirm the stability for one vortex solution of the equation at $h_e = H_{c1}$ on our simulation program. The discretization of the system with the cell size $(a = 2)$ gives convergent solutions in the cases treated in this paper.

III. COMPUTER SIMULATIONS

Let us first examine the time development of the superconducting state by integrating the TDGL equation starting with the normal state $(|\Delta| = 0)$. The quenched normal state is a nonequilibrium state below T_c. Thus, the system asymptotically approaches the uniform superconducting state at $h_e = 0$, where $|\Delta| = 1$ and $B_z = 0$. In Figs. 1 and 2, the time dependence of $|\Delta|$ and B_z is shown at $h_e = 0$, respectively. The current distribution $\mathbf{j}$ is also shown in Fig. 3. As seen in Fig. 1, the order parameter grows. However, it is not uniform in space. There exist vortices and antivortices in the process of the nucleation of superconducting state. We have numerically checked that each vortex and antivortex are quantized with the magnetic flux quanta $\pm\Phi_0 = \pm hc/2e$ ($= \pm 25.1$ in the normalized units).

The vortices and antivortices draw together and annihilate. They are also removed from the film edge. Then the system approaches the uniform equilibrium state. We have observed that the superconducting state grows accompanied by the nucleation of vortices and antivortices even without an external magnetic field, since the phase fluctuation of the order parameter occurs more easily than the amplitude. We may understand this fact as follows: The TDGL equation (1) is rewritten in terms of the phase and amplitude of Δ, $\Delta = f \exp(i\theta)$, as

$$\frac{\partial f}{\partial t} = \tfrac{1}{12}[a^2\nabla^2 f + (1 - f^2)f - a^2|\mathbf{p}_s|^2 f] \ ,$$
(12)

$$\frac{\partial \mathbf{p}_s}{\partial t} = \frac{1}{12}\left[a^2\nabla^2\mathbf{p}_s + 2a^2\nabla\left[\mathbf{p}_s \cdot \frac{\nabla f}{f}\right]\right]$$
$$- a^2(\kappa^2 - \tfrac{1}{12})\nabla \times \nabla \times \mathbf{p}_s - f^2\mathbf{p}_s \ ,$$
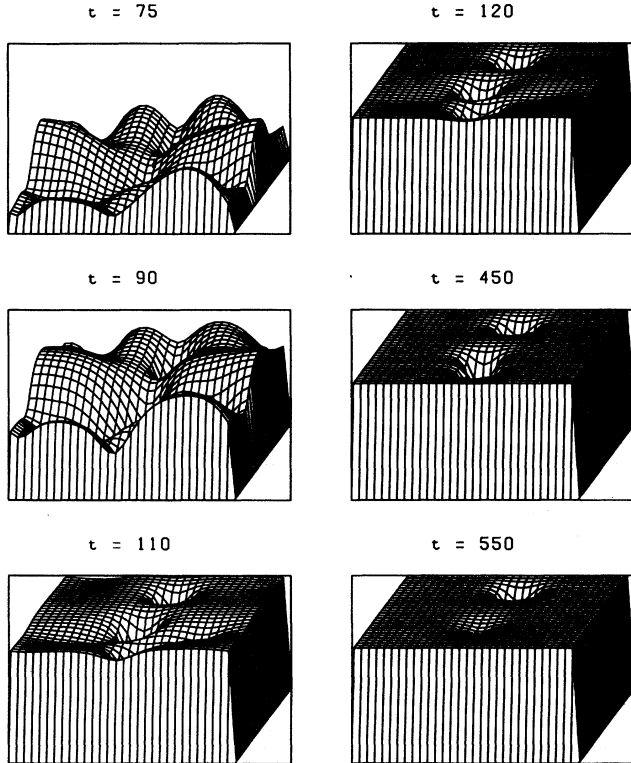
FIG. 1. Time development of the spatial pattern of the order parameter $|\Delta|$ without an external magnetic field $h_e = 0$ at various times. The maximum is normalized to be one.
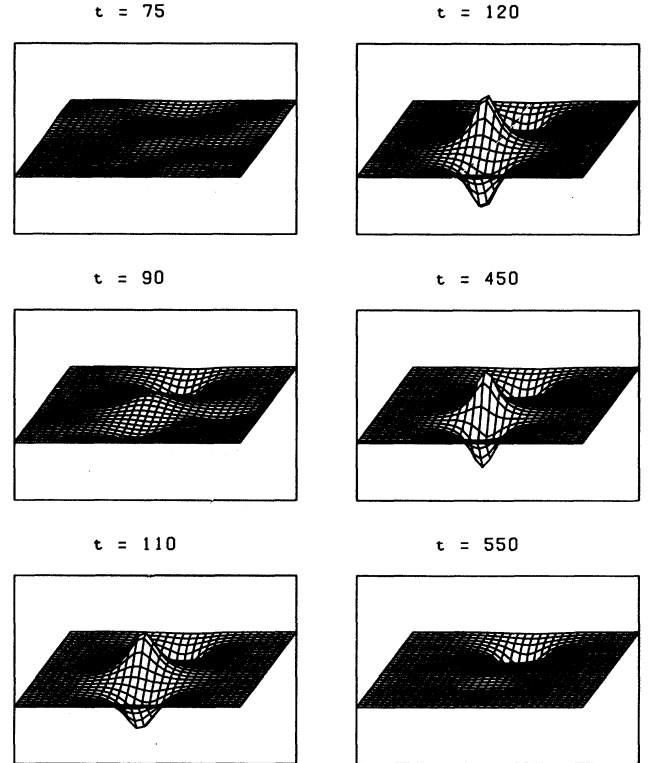
FIG. 2. The spatial pattern of B_z without an external magnetic field $h_e = 0$ at various times. The maximum value of B_z is 0.25 and the minimum value is -0.25.

where $\mathbf{p}_s = \nabla\theta - (\mathbf{A}/a^2)$. The last term in the right-hand side in the first equation has negative sign so that the growth of the amplitude f is depressed by the phase fluctuation. From the last term in the right-hand side of the second equation, we find that once the amplitude grows, the phase gradient is depressed. Then, the system approaches the uniform state at $h_e = 0$.

Let us next apply the external magnetic field $h_e = 0.25$, which is higher than H_{c1} but much smaller than H_{c2}. Thus, the equilibrium state will be the vortex state. Starting with the normal state ($|\Delta| = 0$), we integrate the TDGL equation. The time dependence of $|\Delta|$ is shown in Fig. 4. In this case, the vortex state grows. However, the vortex lattice is not triangular. This is probably because of the effect of the film edge in such a small system used in the calculation. The structure of the vortex lattice also depends on the magnitude of the magnetic field in the small system. The detailed dependence of the structure on the field and the system size will be left to a separate publication. We concentrate on the dynamics in this paper.

Effects of an impurity on a vortex are examined. Here, an impurity exists at a certain point in the film, where the
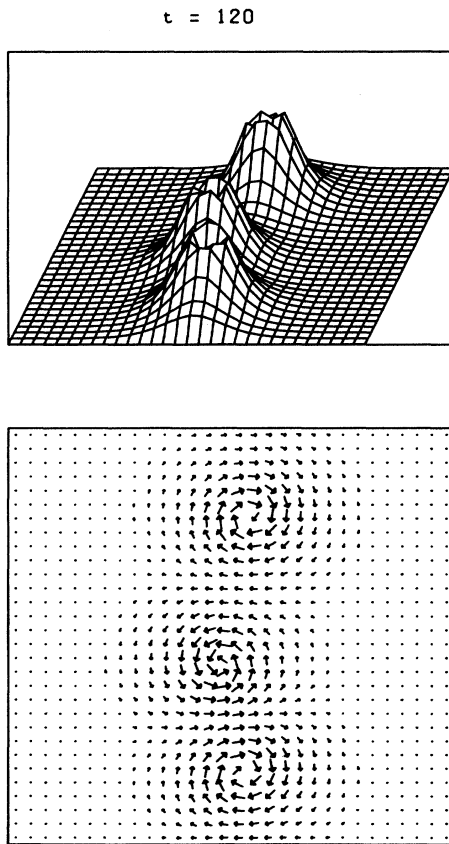
t = 120

FIG. 3. The upper and lower figures show the current distribution $\mathbf{j}$ without an external magnetic field at $t = 120$. The maximum value of $|\mathbf{j}|$ is 0.04. The arrows in the lower figure indicate the direction and magnitude of the current density.

t = 90   t = 250

t = 120   t = 4750

t = 150   t = 10000
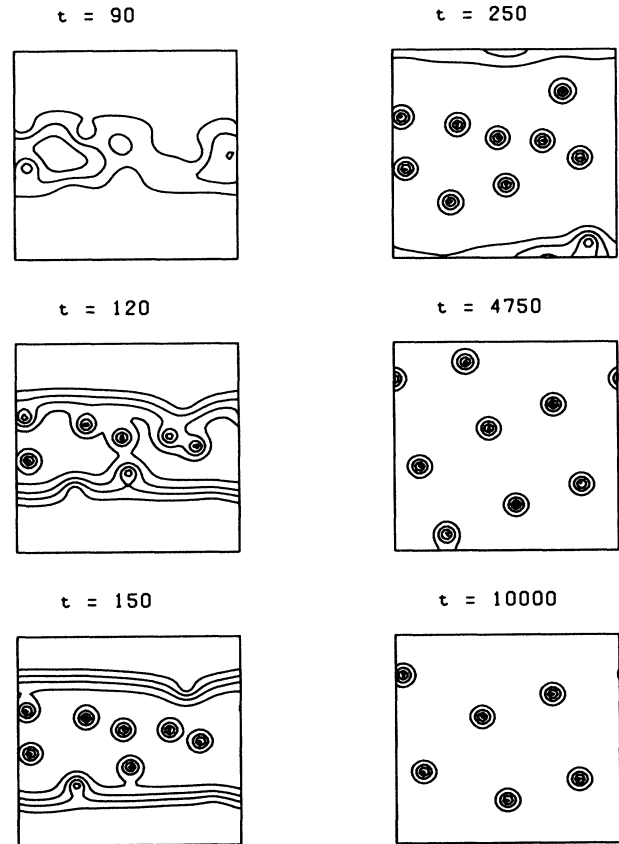
FIG. 4. Time development of the spatial pattern of the order parameter $|\Delta|$ at $h_e = 0.25$. The contour lines with the interval 0.2 are shown at various times. The maximum value is normalized to be one.

t = 5000   t = 14250

t = 14000   t = 15000
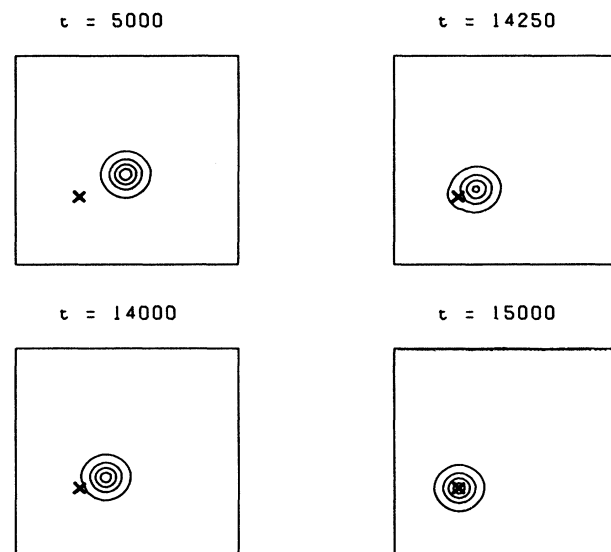
FIG. 5. The spatial pattern of B_z at $h_e = 0$ in the presence of a pinning center denoted by the symbol $\times$. The contour lines of B_z with the interval 0.05 are shown at various times.
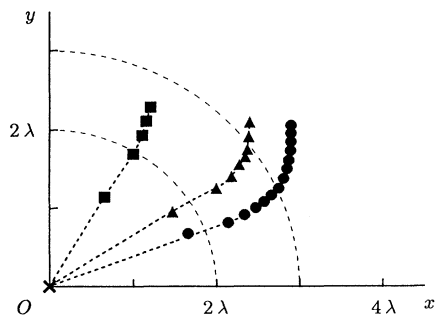
FIG. 6. Trajectories of a vortex when it starts moving to the $-y$ direction at three different points, respectively. The position of a pinning center denoted by the symbol $\times$ is taken to be the origin. The symbols $\blacktriangle$ and $\bullet$ denote the position of the vortex with the time interval $t = 1000$ and the symbols $\blacksquare$ denote that with the time interval $t = 250$. The vortex is quickly trapped by the pinning center once the distance between the vortex and the center becomes less than 2λ.

order parameter is zero. We create a vortex in a magnetic field above H_{c1} and then turn off the field. Since the vortex is not stable at $h_e = 0$, it will be removed from the film edge or it will be trapped by the pinning center. Let a vortex sit on a certain point which is far from the pinning center at $t = 0$ and move to the $-y$ direction with an initial velocity. In Fig. 5, the time dependence of the spatial pattern of B_z at $h_e = 0$ in the presence of a pinning center, denoted by the symbol $\times$, is shown, where the contour lines of B_z with the interval 0.05 are given at several choices of time. We find that the vortex distorts near the pinning center and is trapped by it. In Fig. 6, the trajectories of a vortex in three cases are shown where the vortex sits on three different points at $t = 0$, respectively. The vortex moves to the $-y$ direction with a certain initial velocity in each case. When the distance be-

tween the vortex and the pinning center is less than 2λ, the vortex becomes drawn by the center. In the figure, the symbols $\blacktriangle$ and $\bullet$ denote the position of the vortex with the time interval $t = 1000$ and the symbols $\blacksquare$ denote that with the time interval $t = 250$. We find in the figure that the vortex accelerates near the center.

IV. DISCUSSION AND CONCLUSION

We have proposed a method for studying the superconducting properties based on the numerical integration of the TDGL equation. This method is applied to obtain the static as well as dynamical properties of the superconductors. We demonstrated the simulations of the time development of the superconducting state in the thin film with and without an external magnetic field. We also presented the interaction between a vortex and a pinning center.

Let us consider a superconductor with $T_c = 10$ K. At $T/T_c = 0.9$, for example, t_{GL} is equal to $\sim 10^{-12}$ sec. Thus, a vortex at the distance 2λ from the pinning center is trapped in $\sim 10^{-9}$ sec as seen in Fig. 4. The average velocity of vortex is $\sim 10^5$ cm/sec. The nucleation and annihilation processes of vortices shown in Figs. 1 and 2 also occur in the time range $\sim 10^{-9}$ sec.

In the present paper, we have simulated a few cases. Further simulations by changing the parameters are thus needed. For example, in the case with large κ, we expect an acceleration of the regularization of the vortex lattice because of the large effective interaction compared with the low-κ case.

We have presented computer simulations of the dynamics of the order parameter. This method is applied to simulations of the static and dynamical behaviors of systems with various conditions, such as those with dislocations, inhomogeneous fields, and thermal fluctuation.

ACKNOWLEDGMENT

[1]J. G. Bednorz and K. A. Müller, Z. Phys. B **64**, 189 (1986).
[2]See, for example, A. P. Malozemoff, in *Physical Properties of High Temperature Superconductors*, edited by D. M. Ginzburg (World-Scientific, Singapore, 1989), Vol. 1, p. 971.
[3]A. Brass and H. J. Jensen, Phys. Rev. B **39**, 9587 (1986).
[4]H. J. Jensen, A. Brass, A. C. Shi, and A. J. Berlinsky, Phys. Rev. B **41**, 6394 (1990).
[5]M. M. Doria, J. E. Gubernatis, and D. Rainer, Phys. Rev. B

41, 6335 (1990).
[6]Y. Enomoto, R. Kato, K. Katsumi, and S. Maekawa (unpublished).
[7]See, for example, M. Tinkham, *Introduction to Superconductivity* (McGraw-Hill, New York, 1975).
[8]C. R. Hu and R. S. Thompson, Phys. Rev. B **6**, 110 (1972).
[9]L. P. Gor'kov and G. M. Eliashberg, Zh. Eksp. Teor. Fiz. **54**, 612 (1968) [Sov. Phys. JETP **27**, 328 (1968)].